POLITECNICO MILANO 1863

SCUOLA DI INGEGNERIA INDUSTRIALE E DELL'INFORMAZIONE

Executive Summary of the Thesis

Direct position control of an industrial robot based on an external tracking system

Laurea Magistrale in Mechanical Engineering - Ingegneria Meccanica

Author: Enrico Bruno Chiappini and Federico Pleuteri

Advisor: Prof. Andrea Maria Zanchettin

Co-advisor: Julian Markus Alexander Blumberg

Academic year: 2022-2023

1. Introduction

Industrial robots are versatile machines, able to cover a wide range of applications, and whose adoption in manufacturing processes is rapidly growing all over the world. In particular, they are envisioned to substitute CNC machines in the processing of lightweight materials, such as aluminum and fiber composite plastics, due to their higher flexibility and reduced costs.

However, their low absolute pose accuracy in position and orientation, due to serial construction, gear backslash, and low structural stiffness, limits their capabilities in operations where high precision is required [5].

The implementation of a robust control logic, based on an external tracking system, aims at improving the industrial robot tool pose and path accuracy, thus allowing their usage for new manufacturing duties. For this reason, a Kalman filter, to reduce measurements' noise, and an optimized fuzzy control logic have been developed.

The work has been carried out on a FANUC M-900iB/700 industrial robot, with the use of the camera tracking system ARTTRACK5 from the company ART GmbH & CO. KG, and a Leica Absolute Tracker AT960 as reference.

2. State of the art

Examples of industrial robot control, based on external tracking systems, are provided by Möller et al. in [4] and [5], where respectively a laser tracker and a camera tracking system are used for providing feedback to the control loop. In both cases, the control logic allowed to improve the precision of the robot tool. The main difference between the two is represented by their measurements reliability and precision, which would eventually affect the actual final precision of the robot. Laser trackers offer better performances, whereas camera systems still need to be optimized. However, the expensiveness of the firsts, the fact they can track only one body at a time, and the fact they cannot be solidly attached to the workspace, make the latter a valid alternative.

Anyhow, the control strategy is the same and works by taking as input the external measurements of the robot pose (in green in Fig. 1), transforming them into the desired reference frame and computing the error of the actual state with respect to the target state (in red) at the end-flange. Starting from the Denavit-Hartenberg model for the six-axes robot and having defined the transformation matrices, some known, and others to be calculated, the error pose becomes as follows:

$$T_{6_G}^{6_A} = (T_0^{6_G})^{-1} \cdot (T_W^0)^{-1} \cdot T_W^C \cdot T_C^S \cdot T_S^{6_A} \quad (1)$$

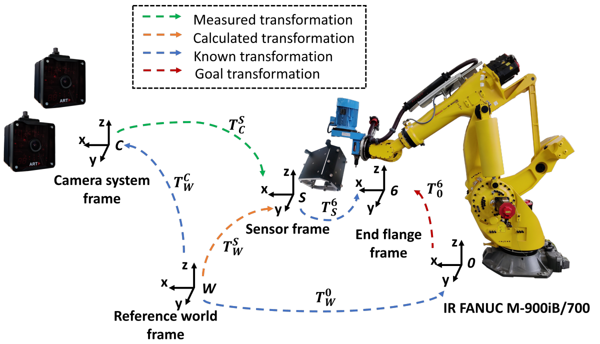

Figure 1: Schematic of reference frames and of transformation matrices

This procedure can be of two types, computing the error in joint space or in Cartesian space. The former can be more effective, since it allows considering each joint as a Single-Input Single-Output system, at the cost of additional transformation between the measured data and the joint reference system, by involving the inverse kinematic model of the robot.
Cartesian space, on the other hand, offers a more direct approach, since it does not involve the inverse kinematic model. However, the system becomes Multi-Input Multi-Output, since each Cartesian movement is the results of the sum of each individual joint rotation.

3. System description

The industrial robot used for conducting the work is an M-900iB/700 by the company FANUC K.K., Oshino, Japan, equipped with a FANUC R-30iB controller. In particular, out of the many functions, the R-30iB controller features the Dynamic Path Modification (DPM) option for real time modification of the robot pose, which enables to dynamically control the end effector position. This function allows to directly apply offsets to the end-flange in Cartesian space, while no direct option regarding the joint space control is available [1].
The external measuring system used is the optical tracking system ARTTRACK5, from the company Advanced Realtime Tracking (ART) GmbH & CO. KG, Weilheim, Germany. The setup consists of four infrared cameras, fixed on the protective cage surrounding the robot, and of a specific target mounted on the robotic arm in the proximity of the tool, which can be recognized by the cameras for estimating the position and orientation.
The communication with the robot and the tracking system is made possible by the *FaRoC* Python library, developed by Wael Hojack in his master's thesis [2]. This enables, through *TCP/IP* protocol, the connection between an external PC and the industrial robot controller, allowing to read data and write variables.
Moreover, it also permits running programs, sending input signals to the robot through DPM, and reading tracking system data, via dedicated *UDP* servers. Within this library, the control logic can be implemented, and the control action can be computed by the external PC at each time instant, from the pose error obtained using the data from the cameras and the ones from the robot, thus providing the output offset.

4. Methodology

4.1. Parameter identification

Experimental tests have been conducted in order to identify the system transfer function (TF), from the applied offset to end-flange displacement, and its related parameters. To do so, a step response analysis has been performed, considering several robot poses within its working space, where a step input is sent thought each of the control channels and the response is measured by the external tracker. Though, in the Cartesian coordinate systems, each axis motion is not uncoupled, being dependent on the action of more joints, still thanks to robot controller it has been possible to neglect this effect.
Moreover, from the joint angles encoder measures, it had been possible to compute the system delay as the difference between the time instance of the sent input and the start of the joint movement. Additionally, the joint angles' response can be modeled with a first order TF, using the encoder measures.
The arm structure, instead, is approximated with a 2nd order TF, which can be defined by natural frequency and damping ratio. The TF parameters are estimated from the tracking system measured response, and by deriving the robot behavior in each different pose.

Eventually, combining the delays, the joint movement, and the structure, the overall system TF is defined as follows:

$$TF = \frac{\mu}{1+s\tau} e^{-ds} \frac{\omega_0^2}{s^2 + 2\,\zeta\omega_0\; s + \omega_0^2} \tag{2a}$$

$$\text{with } \omega_0 = 2\pi f,\;\; \zeta = \frac{d}{2\pi},\;\; \text{and } \alpha = \zeta\,\omega_0 \tag{2b}$$

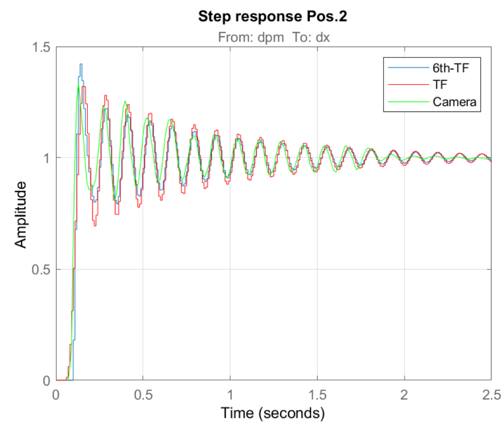

Figure 2: Step response: camera measures and TFs' simulation

The median values obtained for the parameters, over the 14 positions considered for the step response tests, are 7 Hz for the natural frequency f, 0.16 for the damping ratio ζ, 1 for μ, 0.04 for τ and 50 milliseconds for the delay d. Furthermore, each position parameters have been exploited in the implementation of an Extended Kalman filter.

4.2. Static control strategy

Static control is performed by controlling the robot pose around a fixed target in space. A first linear control approach has been done according to the system TF derived from the step response tests. In particular, the DPM function provides a discretized integral action, summing each input to the previously applied offset.
The control action has to work with a minimum sampling time of 15 milliseconds, due to the sampling frequency of the cameras, 150 Hz, and to the additional time needed by the robot controller to apply the input sent.
A linear proportional control logic has been used as benchmark. The system performances have been assessed by perturbing the end effector around the target position, sending step inputs in the control channels. Linear control logics have been developed and tested according to the system TF obtained in the parameter identification phase. Moreover, numerical simulations have been done and confronted with the actual measured responses from the robot, demonstrating similar behavior for low values of the control gains. However, with faster control logics and higher gains, the actual robot response diverges from the theoretical model, showing low frequency oscillations at steady state.
To overcome this problem, a fuzzy control logic has been proposed. Fuzzy logic, is a non-boolean type of logic, where truth values can have varying degree of belonging between zero and one, opposed to Boolean logic. It is useful in control logics for obtaining gain values that gradually change based on the state of the system. Fuzzy logic works according to rules defined on the knowledge of the system and experience.
In the case of the considered industrial robot, the fuzzy logic control has been implemented by taking as input the error magnitude, and giving as output the control gain. The rules set behind the logic has been defined so that bigger output gains are used with big error magnitudes, while switching to lower control gains when close to the target pose. The fuzzy output could then change from the maximum to the minimum linearly, with the optimal gains and error magnitudes determined for each control channel according to the tests results. For instance, the lower control gains are used for error magnitudes below 0.15 millimeters, while above that threshold the gains gradually increased up to the higher values for a faster response.

4.3. Dynamic control strategy

The dynamic control tests have been carried out on a circular path of 1 meter diameter in the horizontal plane, with an inclination of 20 centimeters along the z-axis, to evaluate all the linear axis dynamics. The tests have been conducted with two execution speeds: 60 mm/s (low) and 120 mm/s (high).
Tests have been carried out with proportional control and the already developed fuzzy logic. In both cases, the error with respect to time is noticeably reduced if compared to the uncontrolled trajectory, going from several millimeters to just a few tenths. By comparing the two control strategies, the fuzzy logic allowed to reach a better result, further decreasing the error.

Moreover, as expected, the faster execution speed led to higher errors, while keeping a similar error shape along the trajectory.
Lastly, in addition to the fuzzy control logic, a feedforward control as been added to help to compensate the deterministic part of the error. This strategy has been tested with the lower speed and proved to improve the results.

4.4. Kalman filter

From the dynamic measurements, high frequency oscillations can be noticed in the error values over time, which can be due to noise of the cameras' system. Therefore, to filter out the noisy values from the data measures, a Kalman filter (KF) has been developed and implemented. The second order TF of the structure has been used for describing the system behavior around the target pose, which allowed to design a Simulink model used for an initial concept and tuning phase.
In addition to a more basic Bucy KF (BKF), an Augmented KF (AKF) has been implemented, expanded so to consider also the unknown disturbances and provide proper filtration of the noisy data. Furthermore, Extended Kalman filter (EKF) equations have been used, with non-linear state matrices, for describing the varying dynamics according to the pose.
Therefore, the state-space representation is as follows:

$$\dot{x_a} = \begin{bmatrix} A & E \\ 0 & 0 \end{bmatrix} \begin{Bmatrix} x \\ d \end{Bmatrix} + \begin{bmatrix} B \\ 0 \end{bmatrix} u + \begin{bmatrix} L & 0 \\ 0 & 1 \end{bmatrix} \begin{Bmatrix} wx \\ wd \end{Bmatrix} \tag{3a}$$

$$\boldsymbol{A} = \begin{bmatrix} 0 & 1 \\ -\omega_0^2 & -2\alpha \end{bmatrix}, \ \boldsymbol{E} = \begin{bmatrix} 0 \\ \omega_0^2 \end{bmatrix}, \ \boldsymbol{B} = \begin{bmatrix} 0 \\ \omega_0^2 \end{bmatrix} \tag{3b}$$

$$\boldsymbol{L} = \begin{bmatrix} 0 & 0 \\ 0 & \omega_0^2 \end{bmatrix}, \ \boldsymbol{C} = \begin{bmatrix} 1 & 0 \\ 0 & 1 \end{bmatrix}, \ \boldsymbol{D} = \begin{bmatrix} 0 \\ 0 \end{bmatrix} \tag{3c}$$

with u being the total-applied offset, provided as state variable by the robot controller, x the state of the system (error and error speed), d the unknown disturbances acting along the trajectory, and wx and wd the non-deterministic perturbation of the state.
From the tuning, the optimized values for the diagonal elements of the disturbances' covariance matrix $\boldsymbol{Q}$ result to be [10,100], [10,100,10], and [10,100,100] for the BKF, AKF, and EKF respectively. Even though they apport different filtering effect, the average and maximal error are comparable between them all, arising doubts about the influence of cameras' noise.

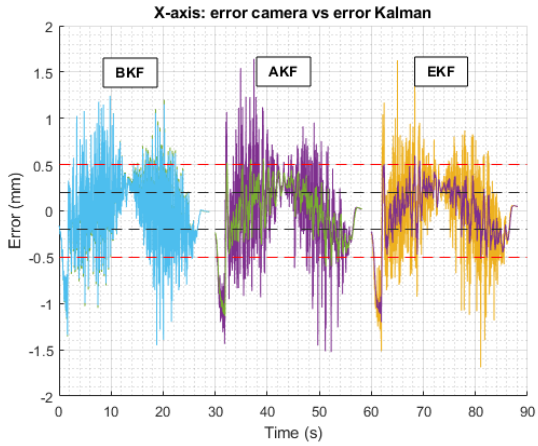

Figure 3: X-error: Kalman comparison

5. Results

Multiple tests have been conducted to measure the system response, in several positions for what concerns the static case, and with different working path for the dynamic one.
The measurements are then compared both with the uncontrolled test and with additional ones provided by the laser tracker.

5.1. Static control results

The static tests have been performed in the same positions used for the parameter identification, as well as six additional random positions within the robot working space.
The system response to input disturbances have been consistent in different positions and along all axes (see example in Fig. 4), quickly reducing the error below the desired threshold, where the lower control gains allow to gradually approach the target.

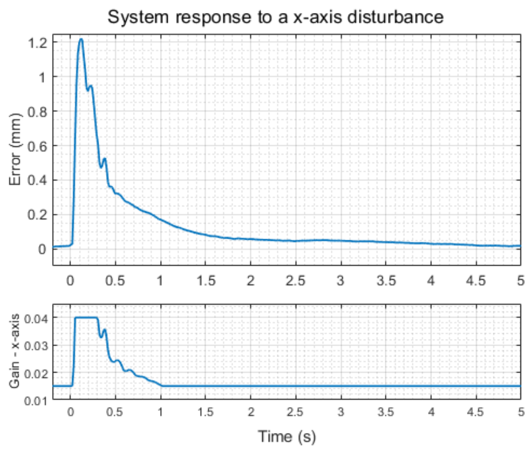

Figure 4: System response to x-axis input

5.2. Dynamic control results

Multiple paths have been used for assessing the dynamic control performances: the circular one used for the control logic development and one derived from the ISO 9283:1998(E) [3]. For each path, execution speeds of 60 mm/s and 120 mm/s have been used. Firstly, the differences between the linear proportional control and the fuzzy logic control has been assessed, with the fuzzy logic showing an improvement for both low and high execution speed.

Table 1: Dynamic circular path control

Error (mm)	1. Linear	2. Fuzzy
Slow		
Median	0.256	0.226
Max	0.673	0.583
Outlier	1.562	1.176
Fast		
Median	0.449	0.392
Max	1.080	0.874
Outlier	2.248	2.160

The data in table 1 refer to the unfiltered measured error with respect to time, used for computing the input offset by the control logic. Fig. 5 shows the error reduction, in comparison between the uncontrolled and controlled test obtained in the circular path travelled at low speed, which reaches peaks up to 96%, by comparing the mean error over a 10% arc length.

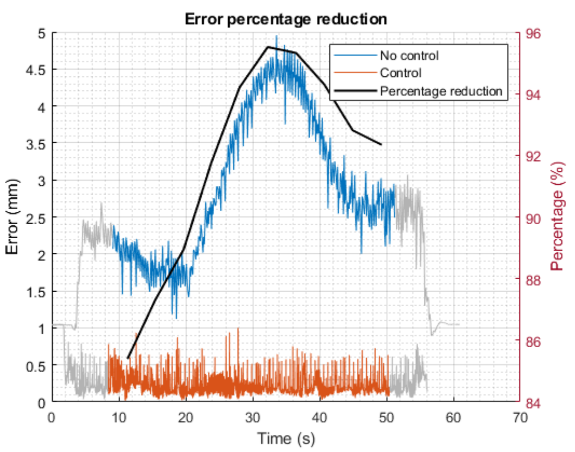

Figure 5: Error reduction in the circular path executed at 60 mm/s

Eventually, the robot precision has been determined by computing the minimum distance between each point of the actual executed trajectory and the target one, without regards to time. The color map in Fig. 7 highlights the critical path areas in the ISO path, such as circular segments and sudden changes in trajectory, where the maximal error is reached, in contraposition to the well controlled straight sections.
High speed show a lower controllability, with similar uncontrolled behavior but higher controlled error, especially in the circular sections, as shown in Fig. 8.

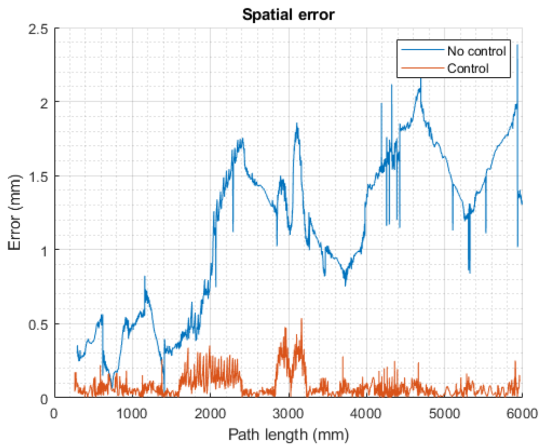

Figure 6: Geometrical error for path derived from ISO at 60 mm/s

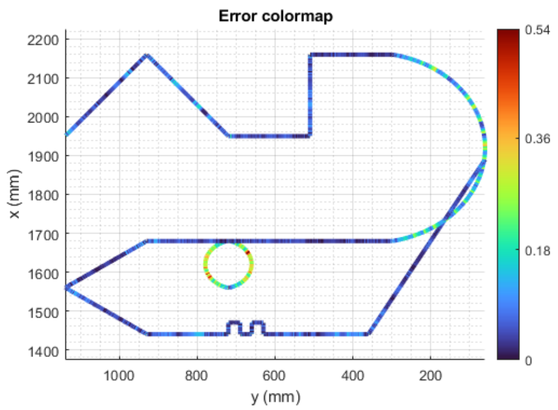

Figure 7: Color map of geometrical error for path derived from ISO at 60 mm/s

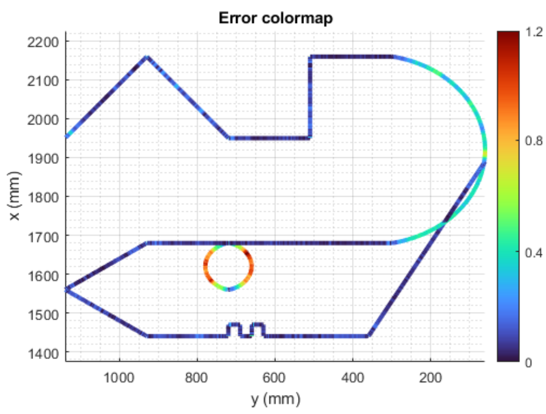

Figure 8: Color map of geometrical error for path derived from ISO at 120 mm/s

6. Conclusions

The pose control of an industrial robot based on an external measuring system, like the camera tracking system used for this work, can represent a relevant improvement for end effector accuracy during both static and dynamic processes. The developed control logic has demonstrated to achieve satisfactory results in different robot poses and trajectories. On the other hand, the exploitation of a Kalman filter did not match expectations, yet improving the results but not showing particular differences between the three implemented types.

In conclusion, the advancements in control due to the developed strategy might allow better manufacturing results, thus increasing the range of applications feasible for industrial robots, in fields where low tolerances are required, thanks to its improved capabilities and robustness.

References

[1] FANUC America Corporation, 3900 W. Hamlin Road, Rochester Hills, Michigan. *FANUC Robot series: R-30iB and R-30iB Plus controller, Dynamic Path Modification, MARUBDPMO02141E*, 11 2021. User's Guide.

[2] Wael Hojak. Entwicklung einer echtzeitfähigen datenschnittstelle sowie einer darauf aufbauenden kamerabasierten echtzeitregelung für industrieroboter. Master's thesis, Technische Universität Berlin, Straße des 17. Juni 135, 10623 Berlin, 3 2023. EN: "Development of a real-time capable data interface and a camera-based real-time control for industrial robots based on it".

[3] *Manipulating industrial robots – Performance criteria and related test methods*, 4 1998.

[4] C. Möller, H. Schmidt, P. Koch, and C. Böhlmann. Real Time Pose Control of an Industrial Robotic System for Machining of Large Scale Components in Aerospace Industry Using Laser Tracker System. *SAE Int. J. Aerosp.*, 2017.

[5] C. Möller, H. Schmidt, N. Shah, and J. Wollnack. Enhanced Absolute Accuracy of an Industrial Milling Robot Using Stereo Camera System. *Procedia Technology*, 26, 12 2016.